ISSN 1070-3284, Russian Journal of Coordination Chemistry, 2017, Vol. 43, No. 9, pp. 612–618. © Pleiades Publishing, Ltd., 2017.

Synthesis, Crystal Structure, and Antibacterial Activity of Oxovanadium(V) Complexes Derived from *N*'-[1-(5-Fluoro-2-Hydroxyphenyl)methylidene]nicotinohydrazide and *N*'-(5-Fluoro-2-Hydroxybenzylidene)-2-Hydroxynaphthylhydrazide[1]

Y. J. Han, L. Wang, Q. B. Li, and L. W. Xue*

College of Chemistry and Chemical Engineering, Pingdingshan University, Pingdingshan Henan, 467000 P.R. China

**e-mail: pdsuchemistry@163.com*

Received September 25, 2016

Abstract—Two new oxovanadium(V) complexes, $[VOL^1(OCH_3)(CH_3OH)]$ (**I**) and $[VOL^2(OCH_3)]$ (**II**), where L^1 and L^2 are the di-anionic form of *N*'-[1-(5-fluoro-2-hydroxyphenyl)methylidene]nicotinohydrazide and *N*'-(5-fluoro-2-hydroxybenzylidene)-2-hydroxynaphthylhydrazide, respectively, have been synthesized and characterized by elemental analysis, FT-IR spectra, and single crystal X-ray determination (CIF files CCDC nos. 891852 (**I**), 891853 (**II**)). The crystal of **I** is monoclinic: space group $P2_1/c$, $a = 8.061(1)$, $b = 15.293(2)$, $c = 13.471(2)$ Å, $\beta = 92.595(2)°$, $V = 1658.8(4)$ Å^3, $Z = 4$. The crystal of **II** is monoclinic: space group $P2_1/n$, $a = 7.4454(9)$, $b = 8.0833(9)$, $c = 28.906(2)$ Å, $\beta = 92.644(2)°$, $V = 1737.8(3)$ Å^3, $Z = 4$. The V atom in **I** is in an octahedral coordination, and that in **II** is in a square-pyramidal coordination. The antibacterial activity of the compounds against various bacteria was assayed.

Keywords: hydrazone ligand, oxovanadium complex, crystal structure, mononuclear complex, antibacterial activity

DOI: 10.1134/S1070328417090020

INTRODUCTION

Vanadium complexes with various types of organic ligands have received remarkable attention in recent years for their biological and medicinal applications [1–4]. Among the wide range of organic ligands, Schiff bases are considered as a very important class of compounds which have been extensively studied on their biological aspects. Some Schiff bases were reported to possess antibacterial, antifungal and antitumor activities [5–7]. Moreover, it is well known that some biological activities, when administered as metal complexes, are being increased [8, 9]. The literature reveals that oxovanadium complexes with hydrazone-type Schiff bases have been less studied. We report herein two new mononuclear oxovanadium(V) complexes, $[VOL^1(OCH_3)(CH_3OH)]$ (**I**) and $[VOL^2(OCH_3)]$ (**II**), where L^1 and L^2 are the di-anionic form of *N*'-[1-(5-fluoro-2-hydroxyphenyl)methylidene]nicotinohydrazide (H_2L^1) and *N*'-(5-fluoro-2-hydroxybenzylidene)-2-hydroxynaphthylhydrazide (H_2L^2), respectively (Scheme 1).

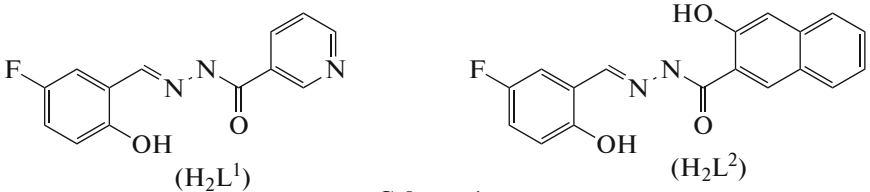

(H_2L^1) (H_2L^2)

Scheme 1.

EXPERIMENTAL

Materials and methods. 5-Fluorosalicylaldehyde, nicotinohydrazide, and 3-hydroxy-2-naphthylhydrazide were purchased from Fluka. Other reagents and solvents were analytical grade and used without further purification. Elemental (C, H, and N) analyses were made on a Perkin-Elmer Model 240B automatic

[1] The article is published in the original.

analyzer. The vanadium content was determined as V_2O_5. IR spectra were recorded on an IR-408 Shimadzu 568 spectrophotometer. Thermal analysis was performed on a Perkin-Elmer Pyris Diamond TG-DTA thermal analyses system.

Synthesis of H_2L^1. 5-Fluorosalicylaldehyde (1.40 g, 0.01 mol) and nicotinohydrazide (1.37 g, 0.01 mmol) were mixed in methanol (30 mL). The mixture was stirred at reflux for 30 min and the solvent was evaporated, to give yellow crystalline product of H_2L^1.

For $C_{13}H_{10}FN_3O_2$

Anal. calcd., %:	C, 60.23;	H, 3.89;	N, 16.21.
Found, %:	C, 60.35;	H, 3.73;	N, 16.12.

Synthesis of H_2L^2. 5-Fluorosalicylaldehyde (1.40 g, 0.01 mol) and 3-hydroxy-2-naphthylhydrazide (2.02 g, 0.01 mmol) were mixed in methanol (30 mL). The mixture was stirred at reflux for 30 min and the solvent was evaporated, to give yellow crystalline product of H_2L^2.

For $C_{18}H_{13}FN_2O_3$

Anal. calcd., %:	C, 66.66;	H, 4.04;	N, 8.64.
Found, %:	C, 66.49;	H, 4.12;	N, 8.73.

Synthesis of $[VO(L^1)(OCH_3)(CH_3OH)]$ (I). H_2L^1 (0.5 mmol, 0.13 g) in methanol (20 mL) was added with stirring to $VO(acac)_2$ (0.5 mmol, 0.13 mg) in methanol (10 mL). The mixture was stirred at refluxed for 30 min to give brown solution. The solution was left still at room temperature in air to give deep brown block-shaped single crystals, which were collected by filtration and dried in vacuum containing anhydrous $CaCl_2$. The yield was 77%.

For $C_{15}H_{15}FN_3O_5V$

Anal. calcd., %:	C, 46.52;	H, 3.90;	N, 10.85;	V, 13.16.
Found, %:	C, 46.37;	H, 3.81;	N, 10.93;	V, 13.32.

Synthesis of $[VO(L^2)(OCH_3)]$ (II) · H_2L^2 (0.5 mmol, 0.16 g) in methanol (20 mL) was added with stirring to $VO(acac)_2$ (0.5 mmol, 0.13 mg) in methanol (10 mL). The mixture was stirred at refluxed for 30 min to give brown solution. The solution was left still at room temperature in air to give deep brown block-shaped single crystals, which were collected by filtration and dried in vacuum containing anhydrous $CaCl_2$. The yield was 69%.

For $C_{19}H_{14}FN_2O_5V$

Anal. calcd., %:	C, 54.30;	H, 3.36;	N, 6.67;	V, 12.12.
Found, %:	C, 54.40;	H, 3.45;	N, 6.73;	V, 12.30.

X-ray diffraction. Data were collected from selected crystals mounted on glass fibers. The data for the complexes were processed with SAINT [10] and corrected for absorption using SADABS [11]. Multi-scan absorption corrections were applied with ψ scans [12]. The structures were solved by direct method using the SHELXS-97 program and refined by full-matrix least-squares techniques on F^2 using anisotropic displacement parameters [13]. All non-hydrogen atoms were refined anisotropically. The hydroxyl hydrogen atom of the methanol ligand in **I** was located from an electronic density map and refined isotropically, with O–H distance restrained to 0.85(1) Å. The remaining hydrogen atoms were placed at the calculated positions. The crystallographic data for the complex are listed in Table 1. Selected bond lengths and angles are given in Table 2.

Supplementary material for structures has been deposited with the Cambridge Crystallographic Data Centre (CCDC nos. 891852 (**I**), 891853 (**II**); deposit@ccdc.cam.ac.uk or http://www.ccdc.cam.ac.uk).

RESULTS AND DISCUSSION

The synthesis of the complexes is shown as Scheme 2:

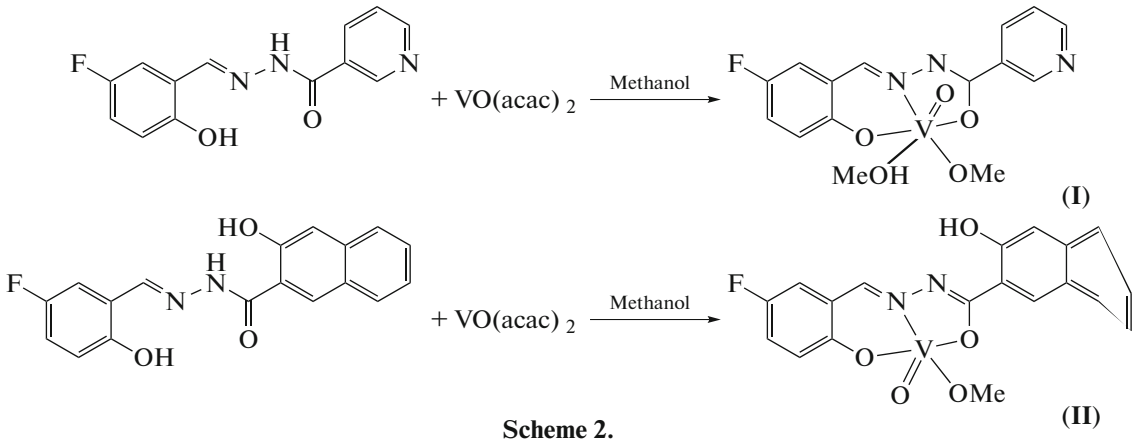

Scheme 2.

Table 1. Crystallographic data and structure refinement summary for the complexes

Parameter	Value	
	I	**II**
Habit, colour	Block, brown	Block, brown
Formula weight	387.24	420.26
Temperature, K	298(2)	298(2)
Crystal size, mm	0.20 × 0.18 × 0.17	0.32 × 0.30 × 0.28
Radiation (λ, Å)	MoK_α (0.71073)	MoK_α (0.71073)
Crystal system	Monoclinic	Monoclinic
Space group	$P2_1/c$	$P2_1/n$
Unit cell dimensions:		
a, Å	8.061(1)	7.4454(9)
b, Å	15.293(2)	8.0833(9)
c, Å	13.471(2)	28.906(2)
β, deg	92.595(2)	92.644(2)
V, Å^3	1658.8(4)	1737.8(3)
Z	4	4
ρ_{calcd}, mg cm^{-3}	1.551	1.606
F(000)	792	856
Absorption coefficient, mm^{-1}	0.640	0.617
θ Range for data collection, deg	2.02–26.45	2.62–25.50
Index ranges	$-10 \le h \le 10$, $-17 \le k \le 19$, $-16 \le l \le 16$	$-9 \le h \le 9$, $-9 \le k \le 9$, $-31 \le l \le 34$
Reflections collected	16499	16517
Independent reflections	3390	3228
Reflections with $I > 2\sigma(I)$	2800	2290
Parameters/restraints	232/1	255/0
Final R indices ($I > 2\sigma(I)$)	0.0351	0.0438
R indices (all data)	0.0924	0.0942
Goodness-of-fit on F^2	1.051	1.044
$\Delta\rho_{max}$, $\Delta\rho_{min}$, e Å^{-3}	0.257, –0.286	0.272, –0.282

The molecular structure of complex **I** is shown in Fig. 1a. The V atom in the complex is in an octahedral coordination, with the phenolate O, imine N, and ethanolate O atoms of L^1 and one deprotonated methanol ligand defining the equatorial plane, and with one oxo O and one methanol O atoms occupying the two axial positions. The V atom deviates from the least-squares plane defined by the four equatorial donor atoms by 0.282(1) Å. The V–O and V–N coordinate bond lengths in the complex are comparable to the corresponding values observed in other similar oxovanadium(V) complexes with hydrazone ligands [14, 15]. The dihedral angle between the benzene ring and the pyridine ring of the hydrazone ligand is 17.2(3)°.

In the crystal structure of complex **I**, molecules are linked through intermolecular O–H···N hydrogen bonds, to form one-dimensional chains along the x axis direction (Fig. 2a). For example, O(5)–H(5)···N(3)^i (^{i} $-1 + x$, y, z): D–H 0.85(1), H···A 1.92(1), D···A 2.751(2), angle D–H···A 173(3)°. In addition, there are also π···π interactions among the chains (Table 3).

The molecular structure of complex **II** is shown in Fig. 1b. The V atom in the complex is in a square pyramidal coordination, with the phenolate O, imine N, and ethanolate O atoms of L^2 and one deprotonated methanol ligand defining the basal plane, and with one oxo O atom occupying the apical position. The V atom deviates from the least-squares plane defined by the four basal donor atoms by 0.472(1) Å. The V–O and V–N coordinate bond lengths in the complex are comparable to the corresponding values observed in other similar oxovanadium(V) complexes with hydra-

Table 2. Coordinate bond distances (Å) and angles (deg) for complexes **I** and **II**

Bond	*d*, Å	Bond	*d*, Å
		I	
V(1)–O(1)	1.8554(14)	V(1)–O(2)	1.9513(13)
V(1)–O(3)	1.5844(16)	V(1)–O(4)	1.7733(15)
V(1)–N(1)	2.1346(17)	V(1)–O(5)	2.2752(15)
		II	
V(1)–O(1)	1.8301(19)	V(1)–O(2)	1.9346(17)
V(1)–O(4)	1.578(2)	V(1)–O(5)	1.757(2)
V(1)–N(1)	2.087(2)		
Angle	ω, deg	Angle	ω, deg
		I	
O(3)V(1)O(4)	101.01(8)	O(3)V(1)O(1)	99.73(7)
O(4)V(1)O(1)	104.45(7)	O(3)V(1)O(2)	99.24(7)
O(4)V(1)O(2)	92.83(6)	O(1)V(1)O(2)	151.27(6)
O(3)V(1)N(1)	92.62(7)	O(4)V(1)N(1)	162.48(7)
O(1)V(1)N(1)	83.77(6)	O(2)V(1)N(1)	73.99(6)
O(3)V(1)O(5)	175.38(7)	O(4)V(1)O(5)	83.49(7)
O(1)V(1)O(5)	78.01(6)	O(2)V(1)O(5)	81.43(6)
N(1)V(1)O(5)	83.16(6)		
		II	
O(4)V(1)O(5)	107.34(11)	O(4)V(1)O(1)	103.96(10)
O(5)V(1)O(1)	98.94(9)	O(4)V(1)O(2)	105.74(9)
O(5)V(1)O(2)	88.71(8)	O(1)V(1)O(2)	145.45(8)
O(4)V(1)N(1)	100.16(9)	O(5)V(1)N(1)	150.86(10)
O(1)V(1)N(1)	83.29(8)	O(2)V(1)N(1)	74.49(7)

zone ligands [16, 17]. There is an intramolecular O–H···N hydrogen bond in the hydrazone ligand, which may lead to the planarity of the ligand with a dihedral angle of 4.1(3)° between the benzene ring and the naphthyl ring. For example, O(3)–H(3)···N(2): D–H 0.82, H···A 1.86, D···A 2.592(3), angle D–H···A 148°. In the crystal structure of complex **II**, molecules are stacked with π···π interactions along the *x* axis direction (Table 3, Fig. 2b).

In the infrared spectra of the free hydrazone ligands, there showed stretching bands attributed to C=O, C=N, C–OH, and NH at about 1663, 1637, 1187, and 3272 cm^{-1}, respectively, for H_2L^1; and at 1660, 1635, 1183, and 3266 cm^{-1}, respectively, for H_2L^2. In the spectra of the complexes, there showed prominent bands at 997 cm^{-1} for **I** and and 978 cm^{-1} for **II**, which attributed to Mo=O bonds. The bands due to ν(C=O) and ν(NH) are absent in the complexes, and the formation of new C–O absorption at about 1239 cm^{-1} for **I** and 1245 cm^{-1} for **II**. This suggests occurrence of keto-imine tautomerization of the ligands during complexation [18]. The –C=N– absorptions observed in the free ligands are shifted to lower wave numbers in the complexes, 1610 cm^{-1} for both complexes.

Figures 3a, 3b are the TG curves of complexes **I** and **II**, respectively. For **I**, the complex undergoes two steps decomposition. The first step started at 170°C and end at 215°C, corresponding to the loss of the methanol ligand. The observed weight loss of 7.8% is in accordance with the calculated value of 8.3%. The second step started at 170°C and end at 475°C, corre-

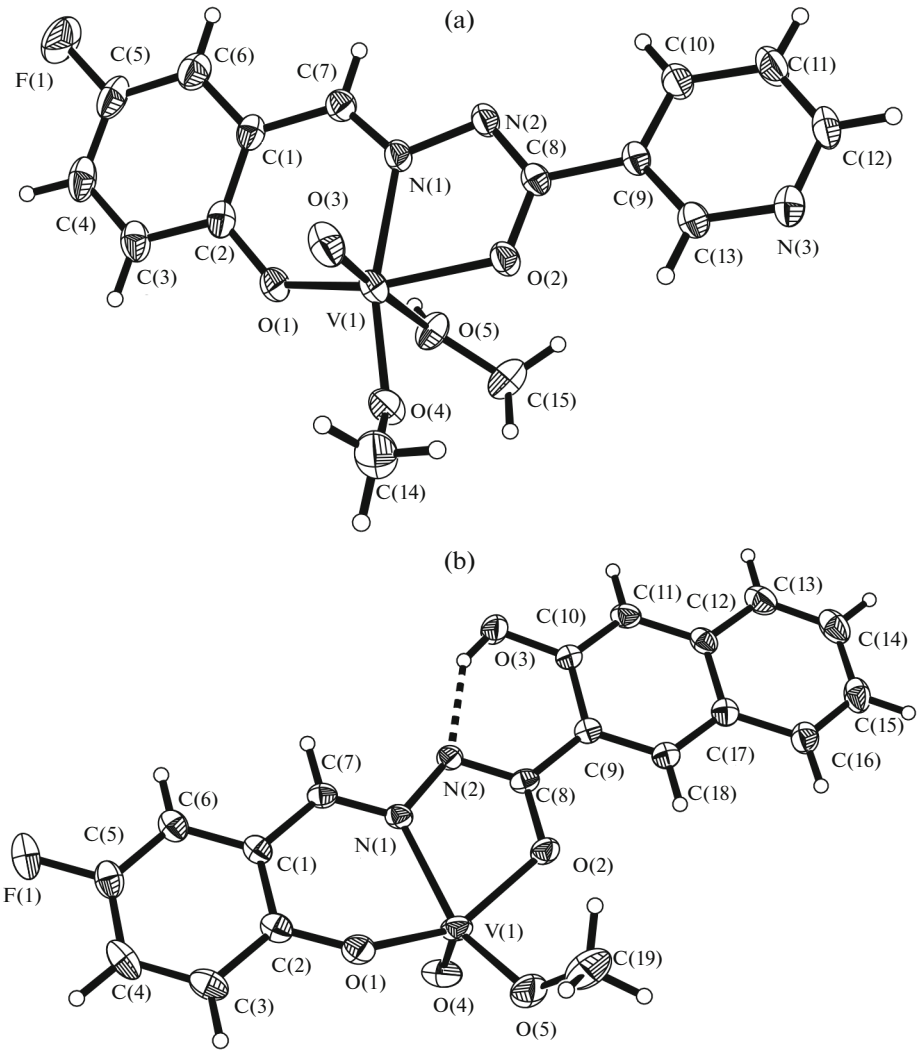

Fig. 1. Molecular structure of **I** (a) and **II** (b) at 30% probability displacement. Hydrogen bond is drawn as a dotted line.

sponding to the loss of the hydrogen ligand and the deprotonated methanol ligand, and the formation of V_2O_5 as the final product. The observed weight loss of 65.7% is close to the calculated value of 64.1%. For **II**, the complex undergoes two steps decomposition. The first step started at 210°C and end at 245°C, corre-

Table 3. π···π Interactions (Å) of complexes **I** and **II**

I			
Cg(1)···Cg(3)^{ii}	4.276(3)	Cg(2)···Cg(3)^{ii}	3.917(3)
Cg(2)···Cg(3)^{iii}	4.821(3)		
II			
Cg(4)···Cg(5)^{iv}	4.161(3)	Cg(4)···Cg(7)^{v}	3.700(3)
Cg(5)···Cg(6)^{vi}	4.438(3)	Cg(5)···Cg(6)^{v}	3.701(3)
Cg(5)···Cg(7)^{vi}	3.854(3)	Cg(5)···Cg(7)^{v}	4.922(3)

Cg(1), Cg(2), and Cg(3) are the centroids of the V(1)–O(2)–C(8)–N(2)–N(1), N(3)–C(12)–C(11)–C(10)–C(9)–C(13), and C(1)–C(6) rings, respectively, for **I**. Cg(4), Cg(5), Cg(6), and Cg(7) are the centroids of the V(1)–O(2)–C(8)–N(2)–N(1), C(1)–C(6), C(9)–C(18), and C(12)–C(17) rings, respectively, for **II**. Symmetry codes: ^{ii} $1 + x, y, z$; ^{iii} $1 - x, -1/2 + y, 1/2 - z$; ^{iv} $x, 1 + y, z$; ^{v} $x, -1 + y, z$; ^{vi} $-1 + x, -1 + y, z$.

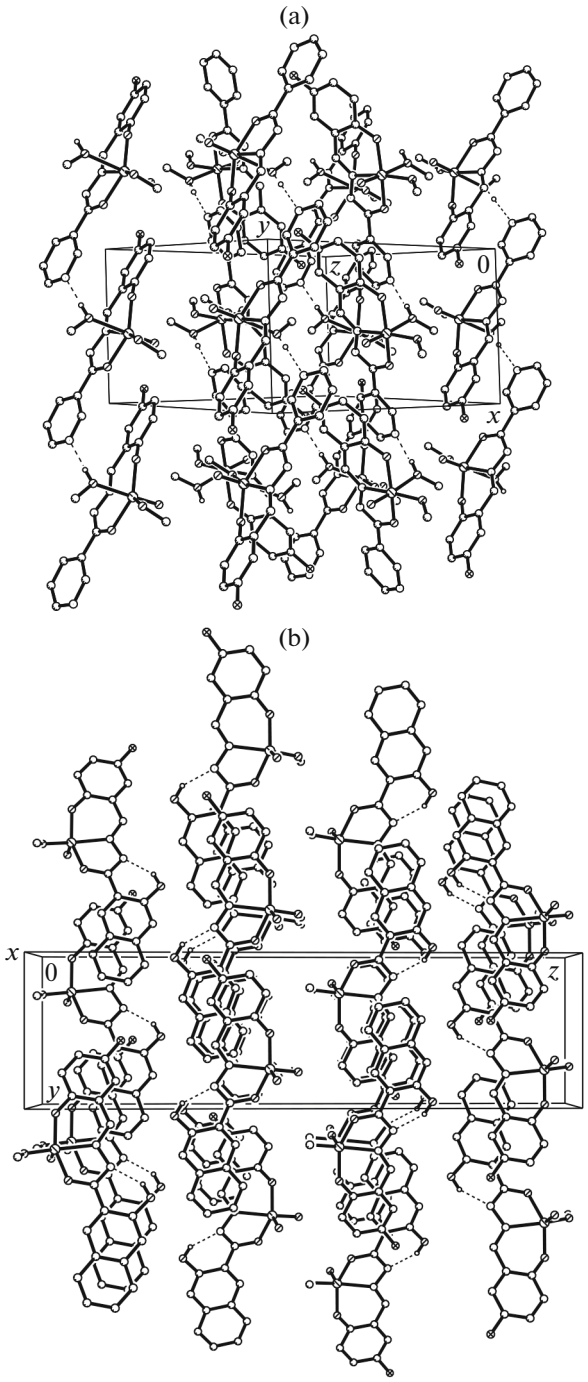

Fig. 2. Crystal packing structure of **I** (a) and **II** (b). Hydrogen bonds are drawn as dotted lines.

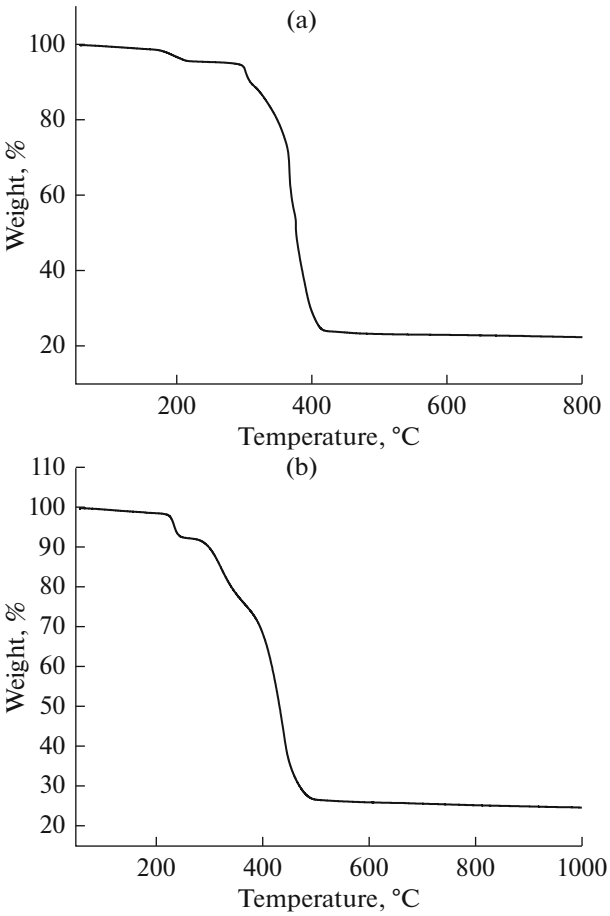

Fig. 3. TG curves of complexes **I** (a) and **II** (b).

sponding to the loss of the deprotonated methanol ligand. The observed weight loss of 7.4% is equal to the calculated value. The second step started at 245°C and end at 490°C, corresponding to the loss of the hydrogen ligand, and the formation of V_2O_5 as the final product. The observed weight loss of 69.3% is close to the calculated value of 71.0%.

Qualitative determination of antibacterial activity was performed using the disk diffusion method [19, 20]. The results are summarized in Table 4. The complexes showed, in general, much more antibacterial activity against *Staphylococcus aureus*, *Escherichia coli*, and *Candida albicans* when compared to the free Schiff base ligands. This might be caused by the greater lipophilic nature of the complexes than the ligands. Such increased activity of the metal chelates can be explained on the basis of chelating theory [21]. On chelating, the polarity of the metal atoms will be reduced to a greater extent due to the overlap of the ligand orbital and partial sharing of positive charge of the metal atoms with donor atoms. Further, it increases the derealization of *p*-electrons over the whole chelate ring and enhances the lipophilicity of the complexes. This increased lipophilicity enhances the penetration of the complexes into the lipid membrane and blocks the metal binding sites on enzymes of microorganisms. It is notable that the complexes have stronger activities than Tetracycline for the bacteria *Escherichia coli* and *Candida albicans*.

Table 4. MIC values (μg/mL) for antibacterial activity of complexes **I** and **II**

Compound	*Staphylococcus aureus*	*Escherichia coli*	*Candida albicans*
H_2L^1	4.0	8.0	256
H_2L^1	8.0	8.0	256
I	4.0	1.0	32.0
II	4.0	1.0	64.0
Tetracycline	0.32	2.12	>512

ACKNOWLEDGMENTS

This research was supported by the National Sciences Foundation of China (nos. 20676057 and 20877036) and Top-class foundation of Pingdingshan University (no. 2008010).

REFERENCES

1. Li, X., Lah, M.S., and Pecoraro, V.L., *Inorg. Chem.*, 1988, vol. 27, no. 25, p. 4657.
2. Monga, V., Thompson, K.H., Yuen, V.G., et al., *Inorg. Chem.*, 2005, vol. 44, no. 8, p. 2678.
3. Rio, D., del Galindo, A., Tejedo, J., et al., *Inorg. Chem. Commun.*, 2000, vol. 3, no. 1, p. 32.
4. Grüning, C., Schmidt, H., and Rehder, D., *Inorg. Chem. Commun.*, 1999, vol. 2, no. 1, p. 57.
5. Sonmez, M., Celebi, M., and Berber, I., *Eur. J. Med. Chem.*, 2010, vol. 45, no. 5, p. 1935.
6. Mohamed, G.G., Omar, M.M., and Ibrahim, A.A., *Eur. J. Med. Chem.*, 2009, vol. 44, no. 12, p. 4801.
7. Sinha, D., Tiwari, A.K., Singh, S., et al., *Eur. J. Med. Chem.*, 2008, vol. 43, no. 1, p. 160.
8. Bagihalli, G.B., Avaji, P.G., Patil, S.A., et al., *Eur. J. Med. Chem.*, 2008, vol. 43, no. 12, p. 2639.
9. Sun, Y.-X., *Synth. React. Inorg. Met.-Org. Nano-Met. Chem.*, 2006, vol. 36, no. 8, p. 621.
10. *SMART and SAINT, Area Detector Control and Integration Software*, Madison: Bruker Analytical X-ray Instruments Inc., 1997.
11. Sheldrick, G.M., *SADABS, Program for Empirical Absorption Correction of Area Detector Data*, Göttingen: Univ. of Göttingen, 1997.
12. North, A.C.T., Phillips, D.C., and Mathews, F.S., *Acta Crystallogr., Sect. A*, 1968, vol. 24, no. 3, p. 351.
13. Sheldrick, G.M., *SHELXL-97, Program for the Refinement of Crystal Structures*, Göttingen: Univ. of Göttingen, 1997.
14. Zhao, Y., Han, X., Zhou, X.-X., et al., *Chin. J. Inorg. Chem.*, 2013, vol. 29, no. 4, p. 867.
15. Monfared, H.H., Alavi, S., Bikas, R., et al., *Polyhedron*, 2010, vol. 29, no. 18, p. 3355.
16. You, Z.-L., Shi, D.-H., Zhang, J.-C., et al., *Inorg. Chim. Acta*, 2012, vol. 384, p. 54.
17. Zhang, X.-T., Zhan, X.-P., and Wu, D.-M., *Chin. J. Struct. Chem.*, 2002, vol. 21, no. 6, p. 629.
18. Rao, S.N., Munshi, K.N., Rao, N.N., et al., *Polyhedron*, 1999, vol. 18, no. 19, p. 2491.
19. Barry, A., In: *Antibiotics in Laboratory Medicine*, Lorian, V., Ed., Baltimore: Williams and Wilkins, 1991, p. 1.
20. Rosu, T., Negoiu, M., Pasculescu, S., et al., *Eur. J. Med. Chem.*, 2010, vol. 45, no. 2, p. 774.
21. Searl, J.W., Smith, R.C., and Wyard, S., *J. Proc. Phys. Soc.*, 1961, vol. 78, no. 505, p. 1174.